ELSEVIER
Available online at www.sciencedirect.com
ScienceDirect
Thin Solid Films xx (2008) xxx – xxx
thin solid films
www.elsevier.com/locate/tsf

Optical characterization of HfO_2 by spectroscopic ellipsometry: Dispersion models and direct data inversion

Jordi Sancho-Parramon [a,*], Mircea Modreanu [b], Salvador Bosch [c], Michel Stchakovsky [d]

[a] *Ruđer Bošković Institute, Bijenička 54, Zagreb 10000, Croatia*
[b] *University College Cork, Tyndall National Institute (TYNDALL), Lee Maltings, Prospect Row, Cork, Ireland*
[c] *Universitat de Barcelona, Martí i Franquès 1, Barcelona 08930, Spain*
[d] *HORIBA Jobin Yvon, Thin Film Division, Chilly-Mazarin 91380, France*

Abstract

Hafnium oxide (HfO_2) has attracted much interest as high-*k* material of choice for gate oxide replacement in future CMOS technologies and for its use in optical coating technology. The determination of optical properties, like refractive index and bandgap, is focus of intense research, since the optical constants of HfO_2 depend on the physical microstructure and the deposition methods and conditions. In the present study optical characterization of very thin HfO_2 films deposited by plasma ion assisted deposition and annealed at different temperatures is carried out. The characterization is performed using ellipsometric measurements in the spectral range from 1.5 to 8 eV and by using the Tauc–Lorentz and Cody–Lorentz dispersion models. In addition, direct inversion of the ellipsometric data is also carried out. The combination of the Cody–Lorentz model with Urbach tail results in the best description of the data and enables to determine meaningful parameters. On the other hand, the direct data inversion is shown to be useful to provide additional information like the presence of subgap absorption peaks and points out features associated to the crystallinity of the material.
© 2008 Elsevier B.V. All rights reserved.

Keywords: Hafnium oxide; Spectroscopic ellipsometry; Optical properties; Tauc–Lorentz; Cody–Lorentz

1. Introduction

Hafnium dioxide (HfO_2) is one of the most promising candidates to replace silicon dioxide (SiO_2) as gate oxide in CMOS technology, due to its high dielectric constant and thermal stability in contact with silicon [1]. Besides, since HfO_2 is transparent down to approximately 250 nm, it has been used as high refractive index material in UV and visible interferential coatings [2]. Other applications of HfO_2 are found in gas and magnetic sensors [3,4]. Due to this high technological interest, a lot of research efforts have been conducted in order to connect the physical properties of the material with the manufacturing conditions, aiming to find the optimal deposition process and parameters for a given application.

One of the most useful techniques in HfO_2 characterization is spectroscopic ellipsometry (SE). This technique is generally used to obtain an accurate determination of HfO_2 films optical properties such as refractive index, absorption coefficient and bandgap [5] or as a metrology tool for thickness determination of very thin HfO_2 films [6]. In addition, it has been shown that the shape of the dielectric function above the bandgap is correlated with HfO_2 crystallinity, enabling the use of SE as structural characterization tool [7]. SE has been also suggested as a way to detect film defects by analysis of small absorption features below the HfO_2 bandgap [8].

Successful application of SE requires an appropriate modelling of the sample under investigation. In particular, the availability of a dispersion model that can flexibly account for the energy dependence of material optical properties is a critical issue. In this paper, the suitability of Tauc–Lorentz and Cody–Lorentz dispersion models for describing ellipsometric spectra of HfO_2 films is analyzed. Samples with different film thickness and annealed at different temperatures are characterized with these models. The validity and limitations of the models are assessed by statistical evaluation of fitting quality,

* Corresponding author.
E-mail address: j.sancho.parramon@gmail.com (J. Sancho-Parramon).

0040-6090/$ - see front matter © 2008 Elsevier B.V. All rights reserved.
doi:10.1016/j.tsf.2008.04.007

confidence limits of model parameters and comparison with the results obtained from direct inversion of the ellipsometric measurements.

2. Theory

2.1. Overview of ellipsometric data inversion

Ellipsometric data consists of two magnitudes at each wavelength or photon energy: the ellipsometric angles Δ and ψ or a combination of them, depending on the measurement setup. In the present study the Mueller matrix elements I_s and I_c related to the ellipsometric angles by:

$$I_S = sin2\psi \times sin\Delta \text{ and } I_c = sin2\psi \times cos\Delta \quad (1)$$

are considered. If the only unknowns of the sample properties are the optical constants of the film, it is possible to invert the ellipsometric data to obtain real and imaginary part of the dielectric function (ε_1 and ε_2) or of the complex refractive index (n and k) at each measured wavelength. Generally the film thickness is also unknown, but it can be extracted using the fact that it is constant for all wavelengths or assuming that the material is transparent in a part of the spectral range, extracting then n and thickness instead of n and k [9,10]. However, generally speaking direct data inversion is not practical when more than two unknowns are considered at each wavelength. Moreover, this approach is very sensitive to statistical measurement errors and does not ensure the Kramers–Kronig consistency between the real and imaginary part of the obtained optical constants.

A more general method consists on the modelling of the sample through a set of parameters that completely describes its optical behaviour. Typically, these parameters are the films thicknesses and a set of parameters defining the dispersion of the optical constants (dispersion model) of the materials with unknown optical constant. The optimal values of the parameters are found by minimisation of a merit function, typically the chi-square estimator χ^2:

$$\chi^2 = \frac{1}{2N-P-1}\sum_{i=1}^{N}\left[\left(\frac{I_{s-m_i}-I_{s-c_i}(x_i)}{\sigma_{s-m_i}}\right)^2 + \left(\frac{I_{c-m_i}-I_{c-c_i}(x_i)}{\sigma_{c-m_i}}\right)^2\right] \quad (2)$$

where N is the total number of experimental data points, P the number of parameters modelling the sample, I_{s-m_i} and I_{c-m_i} are the measured quantities at the wavelength x_i, σ_{s-m_i} and σ_{c-m_i} are the associated experimental errors and I_{s-c} and I_{c-c} are the corresponding calculated quantities for the sample model computed using standard thin film computation algorithms [11]. Values of $\chi^2 \leq 1$ indicate that the discrepancy between model calculation and measurements is within the experimental error. Statistical uncertainties of parameters and correlation between parameters can be calculated by computing the second derivatives of χ^2 [12].

2.2. Dispersion models

Among the multiple models that have been developed to describe the optical properties of materials for energies around the bandgap, one of the most versatile is the Tauc–Lorentz (TL) model proposed by Jellison and Modine [13]. The TL model combines the Tauc expression for the band edge onset [14] with the broadening given by the classic Lorentz oscillator [15]. The imaginary part of the dielectric function has the following expression.

$$\varepsilon_2(E) = 0, \quad E \leq E_g$$
$$\varepsilon_2(E) = \frac{AE_0C(E-E_g)^2}{(E^2-E_0^2)^2+C^2E^2}\cdot\frac{1}{E}, \quad E > E_g. \quad (3)$$

where E_g is the bandgap, A the amplitude, E_0 is the peak transition energy, C a broadening term. The Tauc expression for the imaginary part of the dielectric function assumes parabolic bands and a constant momentum matrix for the electronic interband transitions. However, Cody et al. derived an alternatively expression assuming parabolic bands but a constant dipole matrix element, that appears to describe better the absorption onset of some amorphous materials [16]. Based on the Cody expression and the Lorentz oscillator, Ferlauto et al. [17] proposed the Cody–Lorentz (CL) model

$$\varepsilon_2(E) = 0, \quad E \leq E_g$$
$$\varepsilon_2(E) = \frac{(E-E_g)^2}{(E-E_g)^2E_p^2}\cdot\frac{AE_0C}{(E^2-E_0^2)^2+C^2E^2}, \quad E > E_g \quad (4)$$

where E_p is the transition energy between the absorption onset and the Lorentz oscillator. In the same paper, Ferlauto et al. derived an extension of TL and CL models to include absorption below the bandgap, which in amorphous materials is typically observed as the Urbach tail [18]. The combination of the Urbach subgap absorption with the CL model results in the following expression for the dielectric function:

$$\varepsilon_2(E) = \frac{E_1}{E}exp\left[\frac{E-E_t}{E_\mu}\right], \quad E \leq E_t$$
$$\varepsilon_2(E) = \frac{(E-E_g)^2}{(E-E_g)^2E_p^2}\cdot\frac{AE_0C}{(E^2-E_0^2)^2+C^2E^2}, \quad E > E_t \quad (5)$$

where E_t defines the transition energy between the Urbach and CL absorption ranges and E_1 is defined so that ε_2 is continuous at $E=E_t$. The parameter E_μ is the so-called Urbach energy, representing the width of tail states in the forbidden gap and used to quantify the structural disorder of the material. Although originally named Cody–Lorentz, we shall refer to this expression as the Urbach–Cody–Lorentz (UCL) model. For all three models, TL, CL and UCL, the real part of the dielectric function is calculated from the Kramers–Kronig relation:

$$\varepsilon_1(E) = \varepsilon_\infty + \frac{2}{\pi}P\int_0^\infty \frac{\xi\varepsilon_2(\xi)}{\xi^2-E^2}d\xi \quad (6)$$

ARTICLE IN PRESS

that adds one parameter more (ε_∞) to the previous models. Explicit expressions for $\varepsilon_1(E)$ are given in [13,17]

3. Experimental

HfO_2 films of 20 and 40 nm nominal thickness were deposited by plasma ion assisted deposition (Leybold LAB600) on 1 mm thick p-type <1 0 0> silicon substrates. Before deposition standard chemical cleaning of the substrates was performed without the removal of the native oxide (about 2 nm thick). The deposition was performed at substrate temperature of 150 °C and base pressure of 10^{-6} mbar. The argon flow rate was kept at 5 sccm and the oxygen one at 7 sccm. After the deposition the wafers were cut in pieces and annealed in N_2 atmosphere for 3 h at different temperatures in order to induce structural changes on HfO_2 films and study the crystallisation onset [19]. To keep the same notation as in our previous work, the 20 (40) nm-thick HfO_2 films are named Ha1(Hb1), Ha2 (Hb2), Ha3(Hb3), Ha4(Hb4), Ha5(Hb5), Ha6(Hb6) for the as-deposited, annealed at 300, 350, 450, 500, 750 °C samples respectively. SE measurements were performed using a phase modulated spectrocopic ellipsometer (UVISEL-HORIBA Jobin Yvon) in the 1.5–8.0 eV spectral range at 70° angle of incidence. Further details on the samples and measurements can be found in [19]. For the fitting of ellipsometric data, an improved version of NKDMatl software [20], including the TL, CL, and UCL models, has been used.

4. Results and discussion

Samples have been modelled as five phase-system: incident medium (air), surface roughness layer, HfO_2 layer, SiO_2 interface layer and Si substrate. The optical constants of HfO_2 layer have been represented with the TL, CL and UCL models. The surface roughness has been modelled as a 50% mixture of HfO_2 and voids, with optical constants computed according to the Bruggeman effective medium theory [21]. The optical constants of the interface layer and the substrate have been taken from literature. Thus, the parameters describing the sample are the surface roughness thickness (d_R), the HfO_2 film thickness (d_L), the SiO_2 interface thickness (d_I) and the parameters defining the TL, CL, and UCL models.

Table 1 summarizes the results of the data fitting for the 40-nm thick samples. The merit function obtained using the CL model is between 20% and 40% better than with the TL model and using the UCL model the merit function is 4 to 5 times smaller than the one achieved using the CL model. One may argue that since UCL model involves a higher number of parameters (3 thicknesses + 8 dispersion model parameters) than CL (3 + 6) or TL (3 + 5) it might be possible to find numerically good solutions without physical reliability. However, two statistical figures enhance the validity of the results obtained using the UCL model. First, the statistical uncertainties of the parameters (shown in Table 1) are smaller for the UCL model than for TL or CL models. In addition, we have calculated the cross correlation coefficients between each pair of parameters for each sample and model. The cross correlation factor equals to 1 and 0 for fully correlated and completely uncorrelated parameters. The average cross correlation coefficient using the TL, CL and UCL models is 0.70, 0.54 and 0.47. Thus, while UCL model requires higher number of parameters, their values are more precisely found (less statistical uncertainty) and their mutual correlation is lower. Regarding the parameters values, layers thicknesses for all models are within expected values according to the thickness homogeneity through the wafer and possible modifications upon annealing. However, only the UCL model is able to predict a substantial increase in the bandgap for the samples annealed at highest temperatures (Hb5 and Hb6), where a shift of the absorption onset was observed resulting from sample crystallisation [19].

The fact that CL model gives better results than TL indicates that the assumption of constant dipole matrix element instead of constant momentum matrix element is more appropriate to describe the interband absorption onset of HfO_2. In Fig. 1, the discrepancies between simulated and experimental data for each model for sample Hb3 are shown. It can be noticed that discrepancies in the spectral range between 6.5 and 8 eV, in

Table 1
Parameters and merit functions obtained by fitting the ellipsometric spectra of samples with 40 nm thick HfO_2 films using TL, CL and UCL models

	Hb1	Hb2	Hb3	Hb4	Hb5	Hb6
$d_{R\text{-}TL}$ (nm)	2.1 ± 0.6	2.0 ± 0.6	2.0 ± 0.5	3.3 ± 0.5	3.3 ± 0.5	3.1 ± 0.7
$d_{L\text{-}TL}$ (nm)	45.2 ± 2.0	43.9 ± 1.5	42.2 ± 1.2	44.1 ± 1.3	40.6 ± 1.5	47.3 ± 1.9
$d_{I\text{-}TL}$ (nm)	2.9 ± 1.4	3.0 ± 1.3	2.6 ± 1.0	2.8 ± 1.1	3.0 ± 0.1	2.2 ± 1.6
$E_{g\text{-}TL}$(eV)	5.49 ± 0.10	5.49 ± 0.11	5.47 ± 0.11	5.48 ± 0.09	5.86 ± 0.09	5.56 ± 0.12
χ^2_{TL}	2.82	2.51	1.93	1.85	2.59	3.83
$d_{R\text{-}CL}$ (nm)	1.8 ± 0.5	1.76 ± 0.5	1.77 ± 0.4	3.1 ± 0.4	3.0 ± 0.5	2.9 ± 0.7
$d_{L\text{-}CL}$ (nm)	44.9 ± 1.2	43.8 ± 2.3	42.1 ± 0.9	43.8 ± 1.0	40.5 ± 1.3	47.1 ± 1.6
$d_{I\text{-}CL}$ (nm)	3.3 ± 1.1	3.3 ± 2.0	2.8 ± 0.8	3.2 ± 0.9	3.2 ± 1.1	2.5 ± 1.4
$E_{g\text{-}CL}$(eV)	5.27 ± 0.15	5.25 ± 0.18	5.22 ± 0.13	5.28 ± 0.11	5.72 ± 0.13	5.36 ± 0.17
χ^2_{CL}	2.15	1.69	1.20	1.30	1.93	2.90
$d_{R\text{-}UCL}$ (nm)	1.1 ± 0.3	1.4 ± 0.2	1.6 ± 0.2	2.5 ± 0.2	2.4 ± 0.2	2.2 ± 0.4
$d_{L\text{-}UCL}$ (nm)	46.0 ± 1.1	44.2 ± 0.6	42.4 ± 0.6	44.7 ± 1.0	41.2 ± 0.6	46.7 ± 1.0
$d_{I\text{-}UCL}$ (nm)	2.9 ± 1.0	3.3 ± 0.6	2.7 ± 0.5	2.8 ± 0.9	3.0 ± 0.6	3.3 ± 0.9
$E_{g\text{-}UCL}$(eV)	5.3 ± 0.18	5.36 ± 0.14	5.24 ± 0.17	5.34 ± 0.19	5.89 ± 0.14	5.93 ± 0.35
χ^2_{UCL}	0.66	0.55	0.51	0.39	0.44	1.22

Please cite this article as: J. Sancho-Parramon, et al., Optical characterization of HfO_2 by spectroscopic ellipsometry: Dispersion models and direct data inversion, Thin Solid Films (2008), doi:10.1016/j.tsf.2008.04.007

ARTICLE IN PRESS

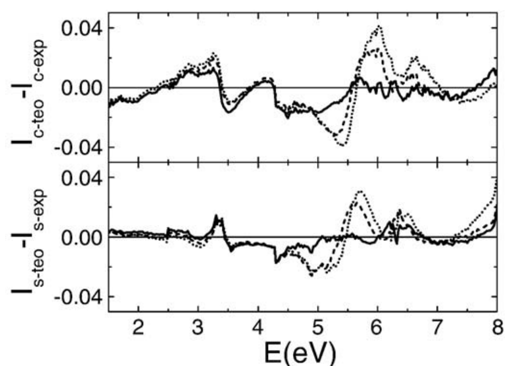

Fig. 1. Discrepancies between experimental and simulated data ($I_{c\text{-teo}}-I_{c\text{-exp}}$, $I_{s\text{-teo}}-I_{s\text{-exp}}$) for sample Hb3s (solid line UCL, dashed CL, dotted TL).

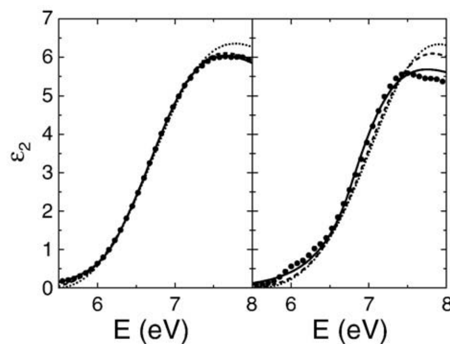

Fig. 3. Imaginary part of the dielectric function obtained from UCL (solid line), CL (dashed line), TL (dotted line) models and from direct data inversion (dots) for Hb3 (left) and Hb6 (right) samples.

which interband transitions takes place, are smaller for CL model than for TL model, suggesting that the first is more appropriate to describe the material properties in this range. However, both CL and TL models present the highest discrepancies from the experiment in the region between 5 and 6 eV. In this spectral range around and below the bandgap, only the UCL model is able to describe properly the experimental data, showing the importance of subgap absorption in the optical properties of the HfO_2 films, which is overlooked by TL and CL models. Apparently the remarkable fitting differences between models by only modifying the absorption in a relatively small spectral range can appear anomalous . However, it must be taken into account that through the Kramer–Kronig relation, the subgap absorption induces changes on the real part of the dielectric function through the whole spectral range. Recently, the sensitivity of ellipsometric measurements to detect Urbach tail absorption has been shown in chalcogenide thin films [22].

For all samples, the discrepancies between UCL model simulation and experimental data are basically equally distributed through the whole spectral range, except for sample Hb6, in which χ^2 is 2–3 times higher than for the other samples. Discrepancies between simulated and experimental data for this sample are shown in Fig. 2. While for the TL and CL model the discrepancies are distributed as stated above, for the UCL model the differences are located in the high energy range (5.5–8 eV). In order to analyze the source of error, we have extracted the real and imaginary parts of the dielectric function of HfO_2 by inverting the ellipsometric data at each wavelength for all samples. For this purpose, the layers thicknesses were fixed to the values found using the UCL model, although there are no significant differences if thicknesses values found with TL or CL models are used. Results for the direct data inversion and comparison with models are shown in Fig. 3, for samples Hb3 and Hb6. For sample Hb3 it can be seen how ε_2 obtained from direct data inversion virtually follows the dispersion of UCL model. However, for sample Hb6, the inverted data shows some specific features at 6 eV and in the range 7.2–8 eV that the UCL model is unable to describe. These particular features are associated to the monoclinic phase of HfO_2 [7] in which sample Hb6 partially crystallised upon annealing [19].

For the samples with 20 nm thick HfO_2 films similar results are obtained: UCL model gave the best fitting for all samples, with χ^2 values ranging from 0.4 to 0.7. In Fig. 4, dielectric function is shown for samples Ha1, Ha5 and Ha6 using the UCL model and from direct data inversion. The absorption edge of HfO_2 in sample Ha6 is shifted towards higher energies with respect to the other samples, which is

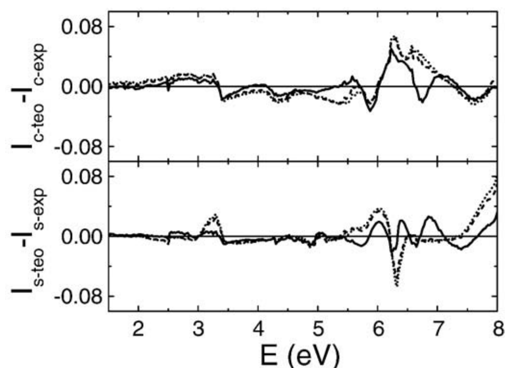

Fig. 2. Discrepancies between experimental and simulated data ($I_{c\text{-teo}}-I_{c\text{-exp}}$, $I_{s\text{-teo}}-I_{s\text{-exp}}$) for sample Hb6s (solid line UCL, dashed CL, dotted TL).

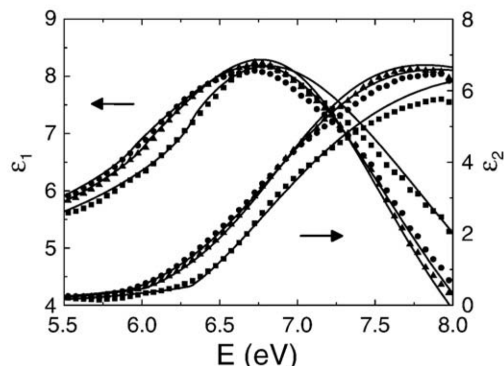

Fig. 4. Real (top) and imaginary (bottom) part of dielectric function of Ha1 (circles), Ha5 (triangles) and Ha6 (squares) samples obtained by direct data inversion and from fitting using the UCL model (solid lines).

Please cite this article as: J. Sancho-Parramon, et al., Optical characterization of HfO_2 by spectroscopic ellipsometry: Dispersion models and direct data inversion, Thin Solid Films (2008), doi:10.1016/j.tsf.2008.04.007

ARTICLE IN PRESS

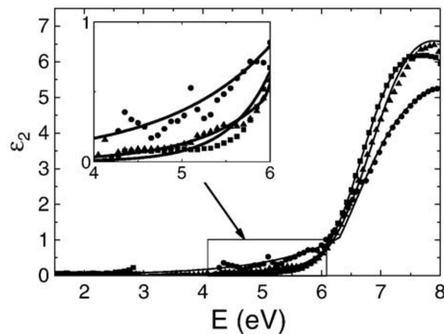

Fig. 5. Imaginary part of the dielectric function for the as-deposited samples with thickness 6 (circles) 20 (triangles) and 40 (squares) nm obtained by data inversion and using the UCL model (solid lines).

related to the crystallisation of the layer upon annealing at 750 °C. However, in opposition to sample Hb6, χ^2 value for Ha6 is not higher for this sample in respect to the other samples of its series. The reason is that Ha6 crystallized crystallised in cubic phase [19], in which the dielectric function does not present specific features like for the monoclinic phase and it can be well approximated by the UCL model. The same stands for sample Hb5, which also crystallized crystallised in cubic phase, but good fitting using the UCL model is obtained.

The Ha sample series show a significant higher absorption below the bandgap with respect to the Hb samples. Data fitting using the TL and CL models, that do not take into account the subgap absorption, led to physically meaningless values of roughness and interface thicknesses. Only when additional TL and CL oscillators are considered to represent this subgap absorption, good fittings were obtained as done in [19,23].

In order to check the thickness dependence of the subgap absorption, an additional 6 nm thick HfO_2 film was investigated. Comparison of the imaginary part of the dielectric function is shown in Fig. 5, where indeed the subgap absorption becomes more remarkable for thinner films similar to the results obtained in [24]. The nature of this subgap absorption is still unclear and has been associated to oxygen vacancies and defects [24,25]. Although these subgap absorption features appear as small peaks below the bandgap, it can be at least partially taken into account through the Urbach tail of the UCL model, enabling the possibility to obtain a good and meaningful data fitting through the whole spectral range.

5. Conclusions

The validity of Tauc–Lorentz (TL), Cody–Lorentz (CL) and Urbach–Cody–Lorentz (UCL) models to describe the optical properties of HfO_2 has been tested on thin films of different thicknesses obtained by plasma ion assisted deposition and annealed at different temperatures. Fitting of ellipsometric spectra of the samples in the spectral range between 1.5 and 8 eV showed that the CL describes better the data than the TL model, suggesting that the constant dipole matrix is a better approximation than the constant momentum matrix to describe the interband absorption onset of HfO_2. However, the best description of the data is achieved when the UCL model is used, i.e. absorption below the bandgap is taken into account, highlighting the relevance of subgap absorption in HfO_2 films for a complete description of its optical properties. Suitability of UCL model is not only assessed by the obtained merit functions but also by the reduced statistical uncertainty and cross correlation of parameters.

The assumption of parabolic bands in which the UCL model is based justifies its appropriateness for amorphous HfO_2 films. By direct data inversion it has been shown that also HfO_2 films in cubic phase can be well described by this model. However, the specific shape that the dielectric function presents for the monoclinic phase of HfO_2 cannot be detected by the model. Direct data inversion also showed that the Urbach tail of the UCL model represents a fair approximation to absorption peaks below the bandgap. Thus, although good data fitting and meaningful parameters can be obtained with the UCL, the detection of small specific features in the dielectric function is better achieved by the direct data inversion.

Acknowledgements

The authors gratefully acknowledge Science Foundation Ireland Grant 05/IN/1751 for the support. JSP thanks the financial support of the Government of Catalonia through a “Beatriu de Pinós” postdoctoral grant.

References

[1] V.V. Afanas’ev, A. Stesmans, F. Chen, X. Shi, S.A. Campbell, Appl. Phys. Lett. 81 (2002) 1053.
[2] P. Torchio, A. Gatto, M. Alvisi, G. Albrand, N. Kaiser, C. Amra, Appl. Opt. 41 (2002) 3256.
[3] S. Capone, G. Leo, R. Rella, P. Siciliano, L. Vasanelli, M. Alvisi, L. Mirenghi, A. Rizo, J. Vac. Sci. Technol. A16 (1998) 3654.
[4] C.L. Platt, B. Dieny, A.E. Berkowitz, Appl. Phys. Lett. 69 (1996) 2291.
[5] M. Modreanu, J. Sancho-Parramon, D. O’Connell, J. Justice, O. Durand, B. Servet, Mater. Sci. Eng. B 118 (2005) 127.
[6] J. Price, P.Y. Hung, T. Rhoad, B. Foran, A.C. Diebold, Appl. Phys. Lett. 85 (2004) 1701.
[7] D. Triyoso, R. Liu, D. Roan, M. Ramon, N.V. Edwards, R. Gregory, D. Werho, J. Kulik, G. Tam, E. Irwin, X.D. Wang, L.B. La, C. Hobbs, R. Garcia, J. Baker, B.E. White Jr., P. Tobin, J. Electrochem. Soc. 151 (2004) F220.
[8] H. Takeuchi, D. Ha, T.J. King, J. Vac. Sci. Technol. A 22 (2004) 1337.
[9] S. Bosch, J. Perez, A. Canillas, Appl. Opt. 37 (1998) 1177.
[10] S. Bosch, F. Monzonis, J. Opt. Soc. Am. A 12 (1995) 1375.
[11] P.H. Berning, Physics of Thin Films, vol. 1, Academic Press, New York, 1963.
[12] G.E. Jellison Jr., Thin Solid Films 290–291 (1996) 40.
[13] G.E. Jellison Jr, F.A. Modine, App. Phys. Lett. 69 (1996), 371; 69 (1996) 2137
[14] J. Tauc, R. Grigorovici, A. Vancu, Phys. Status Solidi 15 (1966) 627.
[15] M. Fox, Optical Properties of Solids, Pergamon Press, Oxford, 1964.
[16] G.D. Cody, in: J.I. Pankove (Ed.), Semiconductors and Semimetals, vol. 21, Academic, Orlando, 1984, p. 11.
[17] A.S. Ferlauto, G.M. Ferreira, J.M. Pearce, C.R. Wronski, R.W. Collins, X. Deng, G. Ganguly, J. App. Phys. 92 (2002) 2424.
[18] F. Urbach, Phys. Rev. 92 (1953) 1324.
[19] M. Modreanu, J. Sancho-Parramon, O. Durand, B. Servet, M. Stchakovsky, C. Eypert, C. Naudin, A. Knowles, F. Bridou, RavetM.F. , Appl. Surf. Sci. 253 (2006) 328.

Please cite this article as: J. Sancho-Parramon, et al., Optical characterization of HfO_2 by spectroscopic ellipsometry: Dispersion models and direct data inversion, Thin Solid Films (2008), doi:10.1016/j.tsf.2008.04.007

[20] S. Bosch, J. Ferre-Borrull, J. Sancho-Parramon, Sol. Stat. Elec. 45 (2001) 703.

[21] D.A. Bruggeman, Ann. Phys. 24 (1935) 636.

[22] I. Ohlidal, D. Franta, M. Šiler, F. Vižd'a, M. Frumar, J. Jedelsky, J. Omasta, J. Non-Cryst. Solids 352 (2006) 5633.

[23] Y.J. Cho, N.V. Nguyen, C.A. Richter, J.R. Ehrstein, B.H. Lee, J.C. Lee, Appl. Phys. Lett. 80 (2002) 1249.

[24] F. Ferrieu, K. Dabertrand, S. Lhostis, V. Ivanova, E. Martinez, C. Licitra, G. Rolland, J. Non-Cryst. Solids 353 (2007) 658.

[25] R. Carriles, J. Kwon, Y.Q. An, L. Sun, S.K. Stanley, J.G. Ekerdt, M.C. Downer, J. Price, T. Boescke, A.C. Deibold, J. Vac. Sci. Technol. B 24 (2006) 2160.

Please cite this article as: J. Sancho-Parramon, et al., Optical characterization of HfO_2 by spectroscopic ellipsometry: Dispersion models and direct data inversion, Thin Solid Films (2008), doi:10.1016/j.tsf.2008.04.007